Research article

The inhibitory effects of Orengedokuto on inducible PGE2 production in BV-2 microglial cells

Yoshika Iwata [a], Mariko Miyao [a], Akiko Hirotsu [a], Kenichiro Tatsumi [a], Tomonori Matsuyama [b], Nobuo Uetsuki [a], Tomoharu Tanaka [a,*]

[a] Department of Anesthesia, Kyoto University Hospital, 54 Kawahara-Cho, Shogoin, Sakyo-ku, Kyoto, 606-8507, Japan
[b] Department of Anesthesia, National Hospital Organization Kyoto Medical Center, 1-1 Mukaihata-cho, Fukakusa, Fushimi-ku, Kyoto, 612-0861, Japan

ARTICLE INFO

ABSTRACT

Background and aim: Reactive microglia has been associated with neuroinflammation caused by the production of proinflammatory molecules such as cytokines, nitric oxide, and prostaglandins. The overexpression of these molecules may provoke neuronal damage that can cause neurodegenerative diseases. A traditional herbal medicine, Orengedokuto (OGT), has been widely used for treating inflammation-related diseases. However, how it influences neuroinflammation remains poorly understood.
Experimental procedure: This study investigated the effects of OGT on inflammatory molecule induction in BV-2 microglial cells using real-time RT-PCR and ELISA. An *in vivo* confirmation of these effects was then performed in mice.
Results and conclusion: OGT showed dose-dependent inhibition of prostaglandin E2 (PGE2) production in BV-2 cells stimulated with lipopolysaccharide (LPS). To elucidate the mechanism of PGE2 inhibition, we examined cyclooxygenases (COXs) and found that OGT did not suppress COX-1 expression or inhibit LPS-induced COX-2 upregulation at either the transcriptional or translational levels. In addition, OGT did not inhibit COX enzyme activities within the concentration that inhibited PGE2 production, suggesting that the effect of OGT is COX-independent. The inhibitory effects of OGT on PGE2 production in BV-2 cells were experimentally replicated in primary cultured astrocytes and mice brains. OGT can be useful in the treatment of neuroinflammatory diseases by modulating PGE2 expression.

1. Introduction

Microglia is a type of glial cells that play a central role in the immune response in the central nervous system (CNS) [1]. In response to pathogens, proinflammatory cytokines and cell necrosis factors [2], they alter their morphology, become phagocytic, and release various inflammatory substances such as cytokines, nitric oxide, and prostaglandins [3]. These reactions may be very significant in terms of defense against infections or may be involved in tissue repair. However, these reactions, in excess, may cause tissue damage to the CNS, leading to various diseases [4]. For example, septic encephalopathy [5], neuropathic pain [6], and neurodegenerative diseases [7] have been associated with the microglia. Most of these diseases are clinically difficult to treat, and drug discovery efforts have been targeted on the microglia [8]. However, clinically effective drugs are still unavailable.

A traditional herbal medicine (Kampo medicine), Orengedokuto (OGT) has been clinically used for treating inflammatory diseases [9]. In terms of its mechanism of action, OGT has been shown to inhibit the production of inflammatory molecules including nitric oxide [10] and prostaglandins [11] in various cells. Interestingly, OGT elicits varying effects on different cells in terms of prostaglandin E2 (PGE2) production. In other words, OGT exhibits augmentation of PGE2 production in intestinal mucosal epithelial cells [12] while suppressing PGE2 in macrophage [13] and one of the most abundant chemical ingredients of OGT, berberine, decreases PGE2 in colorectal cancer cells [14]. PGE2 is a key factor in neuroinflammatory and neurodegenerative diseases [15], but it is not clear what action OGT exerts on PGE2 in the CNS. Here we investigate the effects of OGT on the production of inflammatory substances, especially PGE2, using the microglial cell line BV-2.

---

2. Materials and methods

2.1. Cell culture

The BV-2 immortalized mouse cell line exhibits reactive microglia properties phenotypically and functionally [16]. The cell line was originally developed by Dr. V. Bocchini (University of Perugia, Perugia, Italy) and was provided by Dr. Inoue (Kyushu University, Fukuoka, Japan). BV-2 was cultured in Dulbecco's modified Eagle's medium (DMEM, Sigma-Aldrich, MO, USA) containing 10% fetal bovine serum (FBS) and antibiotics (0.1 mg/ml streptomycin, 100 U/ml penicillin).

2.2. Drugs and chemicals

OGT consists of crude ingredients extracted with boiling water from the following four medicinal herbs in the ratio as follows: Scutellariae radix (S. radix), 3.0; Coptidis rhizome (C. rhizome), 2.0; Gardeniae fructus (G. fructus), 2.0; and Phellodendri cortex (P. cortex), 1.5. A three-dimensional high-performance liquid chromatography profile of OGT provided by Tsumura & Co. is shown in Figure 1. Spray-dried extract powders of OGT, prepared by Tsumura & Co., were dissolved in dimethyl sulfoxide (DMSO) at concentrations of 100 mg/ml and homogenized using the ultrasonic homogenizer. After a 100-fold dilution with cell culture medium, sterile filtration (0.22 μm) was performed and added to the media. Extract powders of S. radix, C. rhizome, G. fructus, and P. cortex were prepared by Tsumura & Co. and processed similarly. Berberine was obtained from Cayman Chemical (MI, USA), and Lipopolysaccharide (LPS), E. coli 055:B5, from Sigma-Aldrich. SB203580 was purchased from Adipogen (Lietstal, Switzerland).

2.3. PGE2 in vitro assay

The PGE2 levels in the culture media were determined using enzyme-linked immunosorbent assay (ELISA) kit (#500141; Cayman Chemical) according to the manufacturer's instructions. Briefly, 50 μL of the supernatant of the culture medium with 50 μL PGE2 tracer was put into the plate and incubated for 1 h at room temperature. The wells were emptied and washed with 10 mM phosphate buffer (pH 7.4) containing 0.05% Tween 20 for five times. Then 200 μL of Ellman's reagent was added to the well and incubated in the dark. Following the developing step that lasted for 1 h, the absorbance was read at 405 nm by a microplate reader. A standard curve was prepared simultaneously with PGE2 standard ranging from 0.05 to 6 ng/ml.

2.4. Animals

This study (ID: Med Kyo 09504) was approved by the Animal Research Committee of Kyoto University (Kyoto, Japan). All the experiments were conducted in accordance with the institutional and NIH guidelines for the care and use of laboratory animals. All mice were purchased from Japan SLC Inc., Shizuoka, Japan. Food and water were provided *ad libitum*, and the mice were maintained under controlled environmental conditions (24 °C, 12 h light/dark cycles).

2.5. Primary cultured astrocytes

The primary cultures of cerebral cortical astrocytes were prepared from 1 day-old C57BL/6NCrSlc mice according to a method described previously [17]. The mice brains were removed under sterile conditions, and the meninges were carefully removed. The tissue was dissociated by passing it through a 320 μm nylon mesh with the aid of a rubber policeman. After washing with Hanks' balanced salt solution containing DNaseI, the cells were suspended and passed through a 100 μm nylon mesh. Next, they were plated on a plastic culture flask (density of two brains per flask) in 10 ml tissue culture medium. The tissue culture medium consisted of DMEM supplemented with 10% FBS, 100 U/ml penicillin, and 0.1 mg/ml streptomycin. The cultures were maintained in a humidified atmosphere of 5% CO2 in air at 37 °C. The medium was changed after 3 days and then twice weekly. At the first medium change, the flasks were vigorously shaken to remove oligodendrocytes and their precursors. All experiments were performed in cells at day 14 *in vitro*.

2.6. PGE2 in vivo assay

OGT (4 g/kg) dissolved in sterile water was administered to male BALB/cCrSlc 8 week mice daily for 4 days by oral gavage. The dose of
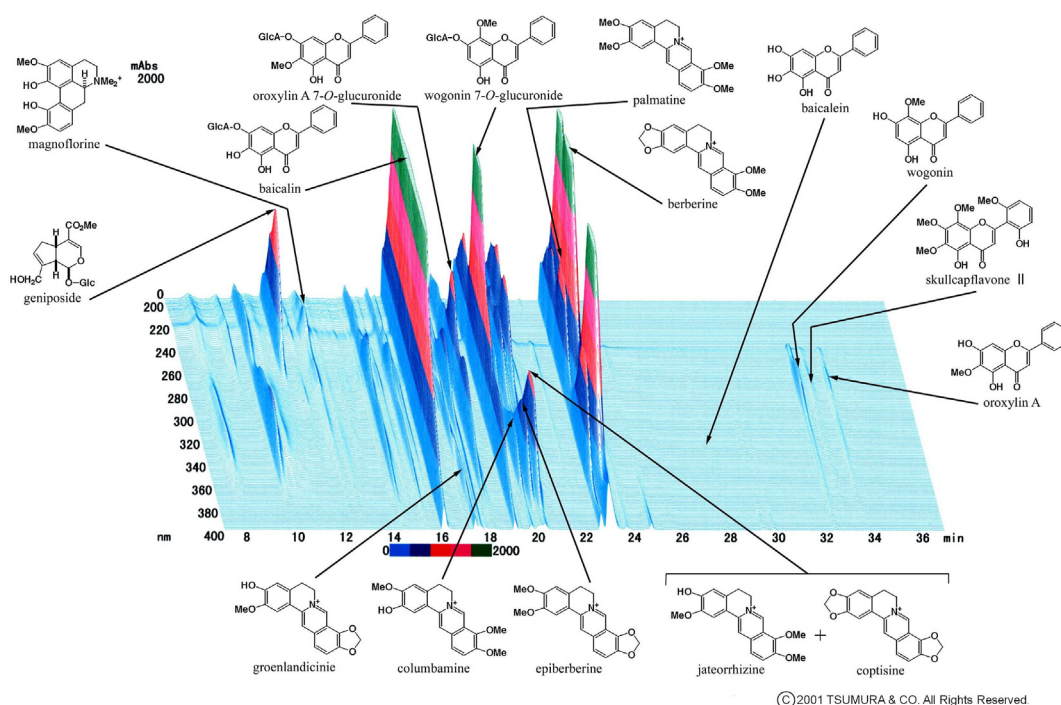

Figure 1. A three-dimensional high-performance liquid chromatography profile of Orengedokuto, provided by Tsumura & Co.

OGT was determined with reference to the past literature [18]. Mice were intraperitoneally injected with LPS (10 mg/kg) and sacrificed by cervical dislocation 3 h after the LPS injection. Then, the whole brains were rapidly harvested and frozen in liquid nitrogen. The entire brain was added to 1 ml of homogenization buffer (0.1M phosphate, pH 7.4, containing 1 mM ethylenediaminetetraacetic acid (EDTA) and 10 μM indomethacin) per gram of tissue and manually homogenized using Dounce grinder. Centrifuged for 10 min at 8,000 xg, the brain homogenates were assayed by an ELISA kit (#500141; Cayman Chemical) according to the manufacturer's instructions. The results were expressed as the ratio of the quantity of PGE2 (in nanogram) to the quantity of total protein (in milligram) in the brain. The total protein concentration was determined by the modified Bradford assay (Nakalai Tesque, Inc., Kyoto, Japan) using bovine serum albumin (BSA) as a standard.

2.7. Real-time quantitative reverse transcription polymerase chain reaction (qRT-PCR)

RNA purification from cultured cells was performed using a Nucleospin® RNA II Kit (Macherey-Nagel, Düren, Germany) according to the description. First-strand cDNA synthesis and RT-PCR were performed with a One Step SYBR™ PrimeScript™ RT-PCR Kit II (Takara Bio, Shiga, Japan) according to the manufacturer's instructions. qRT-PCR assays were performed with a Thermal Cycler Dice Real Time System II (Takara Bio). The PCR primers targeting the mouse genes for 18S rRNA and interleukin (IL)-6 were purchased from Qiagen (Valencia, CA, USA) (Catalog Numbers: 18S, QT02448075; IL-6, QT031168), and primers targeting IL-1β, TNF-α, COX-1, COX-2, cPGES, mPGES1 and mPGES2 were purchased from Invitrogen (CA, USA). Primer sequences are as follows: IL-1β 5′-ATGAGGACATGAGCACCTTC-3′ (forward) and 5′-CATTGAGTTGGAGAGCTTTC-3′ (reverse); TNF-α 5′-TCGTAGCAAAC-CACCAAGTG-3′ (forward) and 5′-CCTTGAAGAGAACCTGGGAGT-3′ (reverse); COX-1 5′-ATGAGTCGAAGGAGTCTCTCG-3′ (forward) and 5′-GCACGGATAGTAACAACAGGGA-3′ (reverse); COX-2 5′-TGAGCAAC-TATTCCAAACCAGC-3′ (forward) and 5′-GCACGTAGTCTTCGATCAC-TATC-3′ (reverse); cPGES 5′-TGTTTGCGAAAAGGAGAATCCG-3′ (forward) and 5′-CCATGTGATCCATCATCTCAGAG-3′ (reverse); mPGES1 5′-GGATGCGCTGAAACGTGGA-3′ (forward) and 5′-CAGGAATGAGTA-CACGAAGCC-3′ (reverse); mPGES2 5′-CCTCGACTTCCACTCCCTG-3′ (forward) and 5′-TGAGGGCACTAATGATGACAGAG-3′ (reverse). For each target mRNA, the fold changes in expression were calculated relative to 18S rRNA.

2.8. Immunoblot assay

Whole cell lysates from cultured cells were prepared using ice-cold lysis buffer [0.1% sodium dodecyl sulfate (SDS), 1% Nonidet P40, 5 mM EDTA, 150 mM NaCl, 50 mM Tris-Cl (pH 8.0), 2 mM dithiothreitol (DTT), 1 mM Na_3VO_4, and complete protease inhibitor (Roche Diagnostics, Bazel, Switzerland)] following a protocol described previously [19]. The total protein concentration was determined by the modified Bradford assay using bovine serum albumin (BSA) as a standard. Aliquots containing 25 μg of protein were fractionated by 7.5%–15% SDS polyacrylamide gel electrophoresis (SDS/PAGE), and the separated proteins were electrotransferred to polyvinylidene difluoride (PVDF) membranes using a transfer buffer. The membranes were probed with the following primary antibodies overnight at 4 °C: β-actin (A5316; Sigma-Aldrich), extracellular signal-regulated kinase 1/2 (ERK1/2) (#4696; Cell Signaling Technology, MA, USA), phospho-ERK1/2 (#4370; Cell Signaling), Jun N-terminal protein kinase (JNK) (#9252; Cell Signaling), phospho-JNK (#9255; Cell Signaling), p38 mitogen-activated protein kinases (MAPK) (#9212; Cell Signaling), phospho-p38 MAPK (#9211; Cell Signaling), COX-1 (#ab695; abcam, Cambs, UK), COX-2 (#AF4198; R&D systems, MN, USA), cPGES (#15216-1-AP; Proteintech, IL, USA), phospho-cPLA2 (#2831; Cell Signaling), and cPLA2 (#2832; Cell Signaling).

Subsequently, the membranes were incubated with horseradish peroxidase (HRP)-conjugated anti-mouse immunoglobulin G (IgG) (GE Healthcare, IL, USA) or anti-rabbit IgG antibodies (GE Healthcare) for 1 h at room temperature. All antibodies were used according to the manufacturer's instructions. Membranes were stripped and reblotted for twice to detect loading controls. Striping maneuver was as below; 5 ml of stripping buffer (stripping buffer component: 40 ml of 10% SDS, 12.5 ml of 1M Tris HCl, pH 6.8, and 146 ml of distilled water) with 40 μl of β-mercaptoethanol was added to PVDF membrane, and the membrane was incubated at 50 °C for 30 min. All chemiluminescent signals were developed with enhanced chemiluminescence reagents (GE Healthcare), and band intensities were quantified using the NIH software Image J Version 1.37.

2.9. Biochemical assay for COX-1 and COX-2 activity inhibition assay

The evaluation of inhibition against cyclooxygenase (COX) activity was carried out using a COX inhibitor screening assay kit (#701230, Cayman) following manufacturer's protocol. Briefly, background tubes (160 μL reaction buffer, 10 μL heme, and 10 μL inactive COX-1 or COX-2), COX 100% initial activity tubes (950 μL reaction buffer, 1 μL heme, and 1 μL COX-1 or COX-2), and COX inhibitor tubes (same content of 100% initial activity tubes) were set up. After setting up the tubes, 10 μL of investigated drug diluted in DMSO was added to COX inhibitor tubes and 10 μL DMSO without drugs to the 100% initial activity tubes. After incubation for 10 min, 10 μL of arachidonic acid was added to all tubes, and the reaction was stopped by adding 30 μL of saturated stannous chloride. The concentrations of prostaglandins (PGs) were quantified using PG enzyme immunoassay provided in the kit. The inhibition of COX-1 and COX-2 activities was measured by comparing the amount of PG produced in inhibitor tube with 100% activity tubes.

2.10. Nuclear protein preparation and trans-AM assay

Nuclear extracts were prepared from BV-2 cells using a nuclear extraction kit (Active Motif, CA, USA). Activation of nuclear factor-kappa B (NF-κB) was quantified using an ELISA-based assay kit (Trans-AM; Active Motif). The assay was performed following the manufacturer's instructions. Nuclear protein (25 μg) was incubated in a 96-well plate coated with oligonucleotides containing the NF-κB consensus site (5′-GGGACTTTCC-3′). The NF-κB content of nuclear extracts binds specifically to this oligonucleotide during incubation for 2 h at room temperature. The NF-κB p65 antibody (100 μl of a 1:1,000 dilution) was then added to each well and incubated for 1.5 h, followed by the addition of 100 μl of HRP-conjugated antibody (1:1,000 dilution) and a further incubation for 1 h. After adding 100 μl of a developing solution, the color was allowed to develop for up to 15 min, and then, the reaction was stopped. The NF-κB activity was determined by reading the absorbance on a spectrophotometer at 450 nm with a reference wavelength of 655 nm.

2.11. Cell viability assay

Cell viability was quantified using a Cell Proliferation Kit I (Roche Diagnostics). BV-2 cells were seeded in a 96-well plate. After 48 h, the cells were treated with OGT for 24 h, and 10 μl of 3-(4,5-dimethylthiazol-2-yl)-2,5-diphenyltetrazolium bromide (MTT) labeling reagent was added to each well, and the samples were further incubated for 24 h in a humidified atmosphere. Then, solubilization solution was added to each well, and the plate was further incubated overnight at 37 °C. A plate reader was used to read the absorption at 590 nm using a reference wavelength of 650 nm. Furthermore, cytotoxicity was evaluated by quantifying the LDH released in culture supernatant from BV-2 cells with damaged membranes, using the CytoTox-96® non-radioactive cytotoxicity assay (Promega, WI, USA) according to the manufacturer's instructions. Detection was performed using a microplate reader at 450 nm.
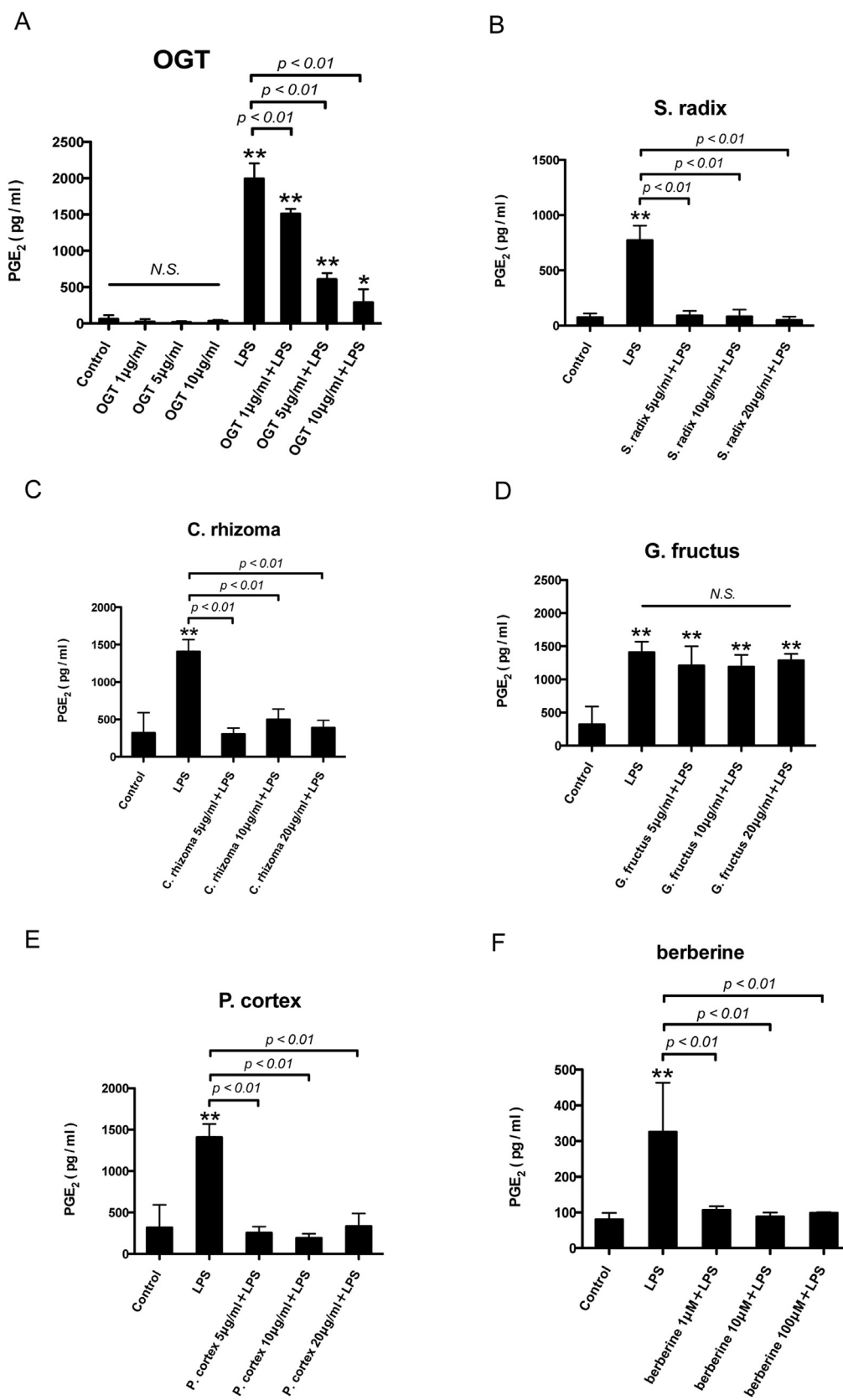
Figure 2. Effects of Orengedokuto (OGT) and its component on PGE2 production in BV-2 cells. BV-2 microglial cells were exposed to OGT (A) or its component, Scutellariae radix (S. radix) (B), Coptidis rhizoma (C. rhizoma) (C), Gardeniae fructus (G. Fructus) (D), Phellodendri cortex (P. Cortex) (E) and berberine (F) for 24 h with lipopolysaccharide (LPS) (1 μg/ml). The level of PGE2 in the cultured media was analyzed by the enzyme immunoassay. Data are shown as mean ± S.D. of three to five independent experiments. **$P < 0.01$ versus control, *$P < 0.05$ versus control, *N.S.*, not significant.

A

MTT assay
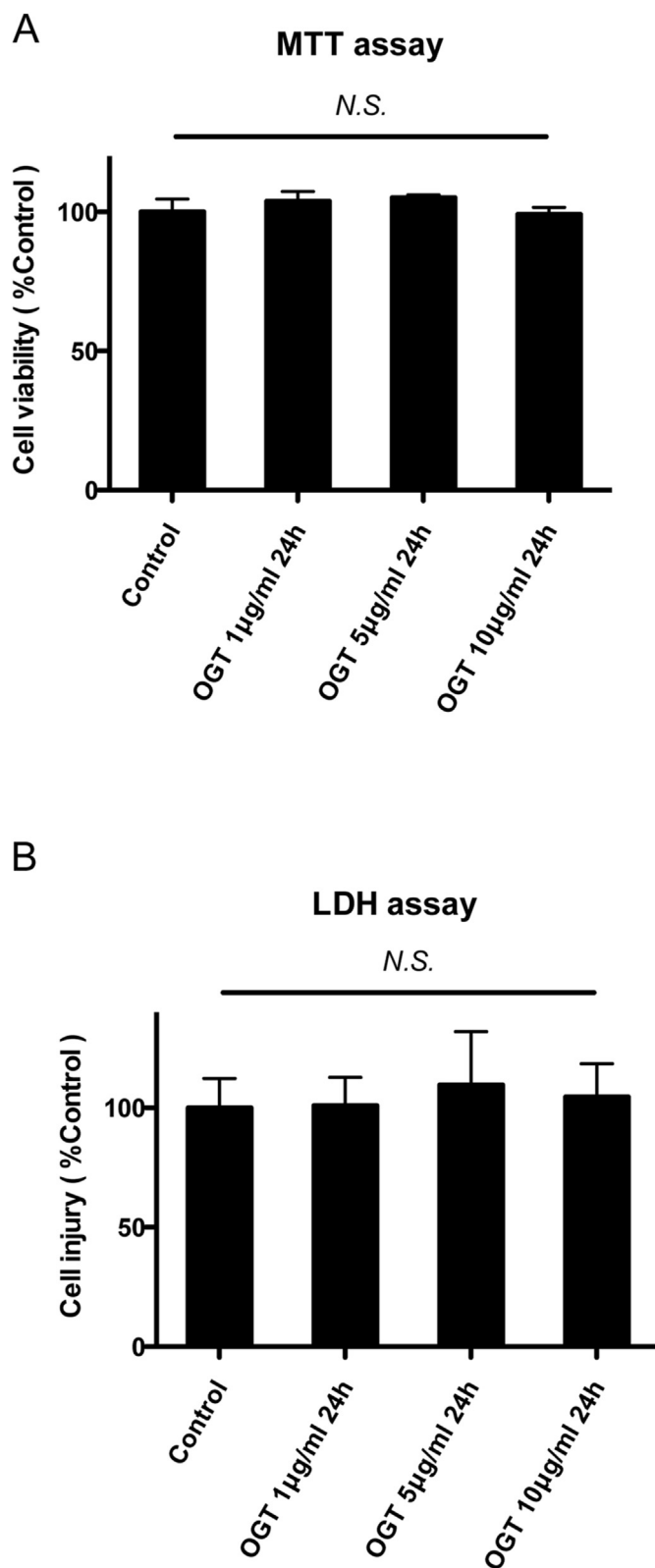
N.S.

B

LDH assay

N.S.

Figure 3. Cytotoxic effects of OGT on BV-2 cells. BV-2 cells were treated with OGT (1, 5, and 10 μg/ml) for 24 h. Cell viability and injury were determined using the MTT (A) and LDH (B) assay. The result was shown as the relative ratio of control. Data are shown as mean ± S.D. of three independent experiments; *N.S.*, not significant.

The activity of the released LDH was reported as a percentage of control. The assay was conducted in triplicates.

2.12. Statistical analysis

Statistical analysis was performed using GraphPad Prism version 5.0 (GraphPad Software Inc., CA, USA), and a *P* value of <0.05 was considered significant. All data of *in vitro* experiments are presented as means ± standard deviation (S.D.) of at least three independent experiments. Values were compared with one-way analysis of variance, followed by the Student–Newman–Keuls test. The data of the *in vivo* experiments were presented as means ± standard error (S.E.), and the values were compared with the Wilcoxon rank sum test.

3. Results

3.1. OGT suppresses PGE2 production in LPS-stimulated BV-2 cells

First, we examined the effect of OGT on PGE2 production in LPS-stimulated BV-2 cells. The results showed that LPS enhanced the production of PGE2, and OGT significantly suppressed it in a concentration-dependent manner (Figure 2A). Without LPS stimulation, OGT did not affect the PGE2 level (Figure 2A). OGT is a mixture of S. radix, C. rhizome, G. fructus, and P. cortex. All ingredients but G. fructus showed PGE2 inhibition in LPS-stimulated BV-2 cells (Figure 2B–E). In addition, one of the most abundant chemical ingredients of OGT, berberine, showed the same PGE2 inhibitory effect (Figure 2F). To exclude the possibility that the cytotoxic effect of OGT could affect the result, we performed MTT and LDH assay and confirmed that at the concentration we examined, OGT did not affect BV-2 cell viability nor show the significant cytotoxicity (Figure 3A,B).

3.2. OGT does not inhibit COX expression and activities in LPS-stimulated BV-2 cells

We examined the mechanism of how OGT suppresses PGE2 production. Freed arachidonic acid is transformed into PGE2 via COX enzymes and prostaglandin E synthase (PGES). Because several drugs including non-steroidal anti-inflammatory drugs (NSAIDs) are known to act on COX, first, we investigated the effect of OGT on COX-1 and COX-2. LPS induced COX-2 expression in transcriptional and translational levels, but OGT did not suppress but rather increased COX-2 expression (Figure 4B, C and E). COX-1 was not influenced by LPS, and OGT did not suppress the expression of COX-1 (Figure 4A, C and D). Conversely, COX enzyme activity assay revealed that OGT did not suppress either COX-1 or COX-2 activity at the concentration of 22 μg/ml but lowered the COX-1 enzymatic activity by 15% at 44 μg/ml (Figure 4F).

3.3. Effects of OGT on PGES expression in LPS-stimulated BV-2 cells

PGESs are enzymes that convert intermediate product PGH2 into end-product PGE2 and are classified into cytosolic type (cPGES) and microsomal types (mPGES1 and mPGES2). mPGES1 are induced by inflammatory stimulation and functionally linked with COX-2 [20]. As shown in Figure 5A, LPS significantly induced mPGES1 and OGT further increased mPGES1 expression. Furthermore, LPS did not influence mPGES2 expression, and OGT rather increased mPGES2 expression (Figure 5B). According to the previous report, cPGES expresses constitutionally and is functionally linked with COX-1 [21]. OGT significantly suppressed cPGES mRNA expression (Figure 5C), but immunoblotting revealed that cPGES expression level was not changed with LPS or OGT (Figure 5D,E).
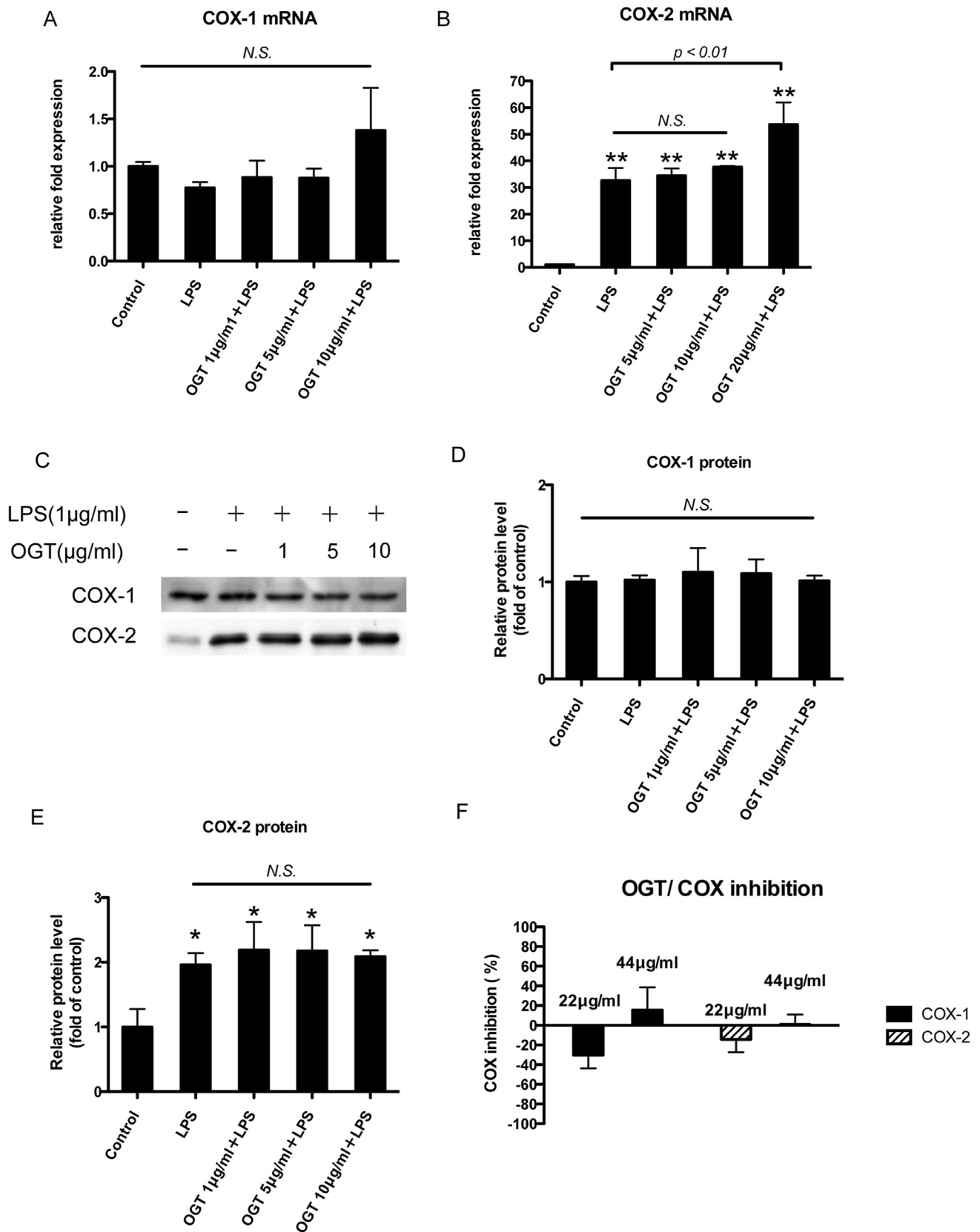
Figure 4. Effects of OGT on COX expression in BV-2 cells. BV-2 cells were exposed to OGT for 24 h with LPS (1 μg/ml). COX-1 (A) and COX-2 (B) mRNA were analyzed using real-time qRT-PCR, normalized to that of 18S rRNA and expressed relative to the mean of control. The data are presented as means ± S.D. of three to five independent experiments. **$P < 0.01$ versus control, *N.S.*, not significant. After 24 h of OGT exposure to BV-2 cells, whole cell lysates were analyzed for COX-1 and COX-2 expression by immunoblot assay (C). The figures are representative of at least three independent experiments. Immunoblot quantification of COX-1/β-actin (D) and COX-2/β-actin (E) are shown. *$P < 0.05$ versus control, *N.S.*, not significant. COX enzyme activity affected by OGT was measured with a cyclooxygenase activity assay kit for COX-1 and COX-2 (F). The data are shown as mean ± S.D. of three independent experiments.
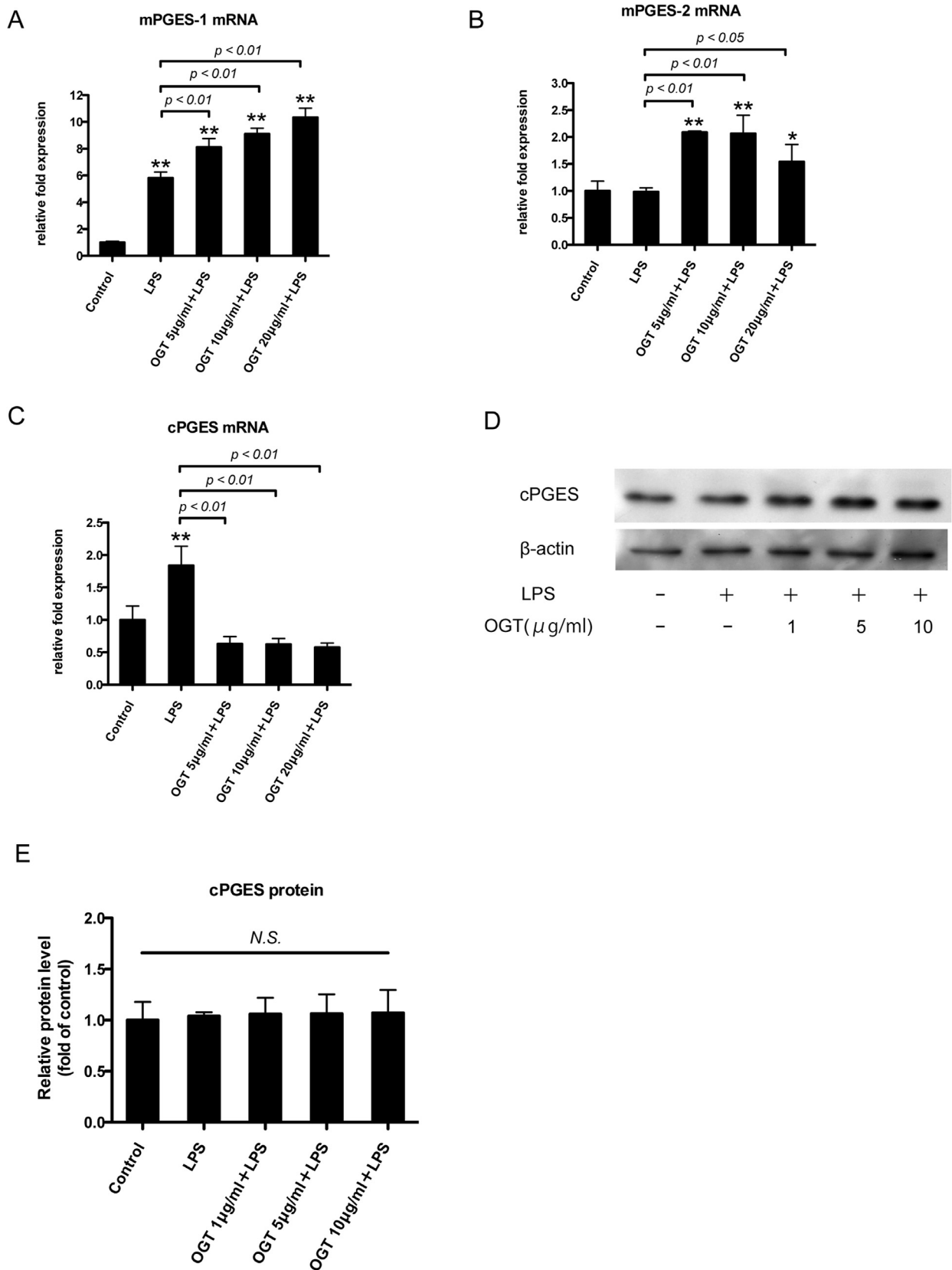
Figure 5. Effects of OGT on PGES expression in BV-2 cells. BV-2 cells were exposed to OGT for 24 h with LPS (1 μg/ml). mPGES1 (A), mPGES2 (B), and cPGES (C) mRNA were analyzed using real-time qRT-PCR, normalized to that of 18S rRNA and expressed relative to the mean of control mice. The data are presented as means ± S.D. of three to four independent experiments. **$P < 0.01$ versus control, *$P < 0.05$ versus control, *N.S.*, not significant. After 24 h of OGT exposure to BV-2 cells, whole cell lysates were analyzed for cPGES and β-actin expression by immunoblot assay (D). The figures are representative of at least three independent experiments. Immunoblot quantification of cPGES/β-actin are shown in E. *N.S.*, not significant.

3.4. OGT suppresses phosphorylation of p38 MAPK in LPS-stimulated BV-2 cells

Arachidonic acid is freed from membrane phospholipids mainly by the cytosolic enzyme phospholipase A2 (cPLA2). cPLA2 was activated through phosphorylation induced by mitogen-activated protein kinase (MAPK). We investigated the effects of OGT on cPLA2 expression and found that OGT did not suppress the expression of phosphorylated and the total form of cPLA2 (Figure 6A-C). Next, we examined MAPK activity in BV-2 cells, which revealed three major MAPK signaling molecules: ERK1/2, JNK, and p38 MAPK. We observed that OGT significantly suppressed phosphorylation of p38-MAPK (Figure 7A,B). Furthermore, OGT increased LPS-stimulated phosphorylation of ERK1/2 at a concentration of 1 μg/ml but decreased at higher concentrations (Figure 7A). To investigate the effect of p38 MAPK on LPS-induced PGE2 production in BV-2 cells, we performed the experiment adopting p38-MAPK inhibitor, SB203580. As shown in Figure 7C, SB203580 significantly suppressed PGE2 production and OGT did not show additive effect with SB203580. On the other hand, SB203580 inhibited COX-2 expression, but the effect was not so distinctive compared with that on PGE2 (Figure 7E).

3.5. Effect of OGT on proinflammatory cytokine expression in LPS-stimulated BV-2 cells

Proinflammatory cytokines including IL-1β, IL-6, and TNF-α are critical inflammatory mediators as well as PGE2. To analyze the effect of OGT on proinflammatory cytokine expression, BV-2 cells were exposed to OGT in the presence of LPS. OGT significantly suppressed IL-1β mRNA induction in a concentration-dependent manner (Figure 8A). But OGT did not suppress IL-6, and rather upregulated TNF-α mRNA induction (Figure 8B,C). NF-κB has been implicated in proinflammatory molecule induction in various cells, including microglia [22]. Therefore, we examined the effects of OGT on NF-κB activity. NF-κB transcription quantified with an ELISA-based kit was significantly elevated with LPS exposure, but OGT did not affect its activation (Figure 8D).

3.6. OGT suppresses LPS-induced PGE2 production in primary cultured astrocytes and mice brains

In the brain, PGE2 is produced not only by microglia but also by astrocytes. We examined whether the PGE2 inhibitory effect of OGT was observed using primary culture astrocytes. OGT significantly suppressed LPS-induced PGE2 production in astrocytes as well as in BV-2 cells (Figure 9A). Finally, it was tested to see if the effect of OGT observed *in vitro* would be confirmed in mice. After the oral administration of OGT to BALB/cCrSlc 8 week mice for 4 days, LPS was intraperitoneally administered to examine the effect on PGE2 in the brain. OGT significantly suppressed the intracerebral PGE2 induction in mice (Figure 9B).

4. Discussion

OGT is one of the basic components of Kampo, a Japanese traditional herbal medicine, used for various diseases involving systemic inflammation and hyperemia [13, 14]. Some clinical trials have shown its effect on hypertension [23]. In the current study, we found that LPS-induced PGE2 production in microglial cultured cells, BV-2, is suppressed by OGT in a dose-dependent manner. Different results have been reported regarding the effects of OGT on PGE2. For instance, OGT significantly increased PGE2 levels in the intestinal mucosa in indomethacin-injected mice and prevented gastrointestinal ulcer formation [12]. However, the induction of PGE2 is suppressed in macrophage-type cultured cells RAW264.7 cells [13]. In the present study, OGT significantly suppressed the LPS-stimulated PGE2 induction in both BV-2 and primary culture astrocytes, but the effect was more distinctive in BV-2 cells. Because microglia is a type of tissue macrophages [1], OGT may have a PGE2 inhibitory effect in macrophage lineage cells.

Considering the mechanism of PGE2 inhibition of OGT, previous study by Li et al. found that OGT reduced COX-2 expression in RAW 264.7 murine macrophages [24]. However, in the present study, OGT did not significantly affect COX-2 expression at the transcriptional or translational levels in LPS-stimulated BV-2 cells. In the study by Li et al.,
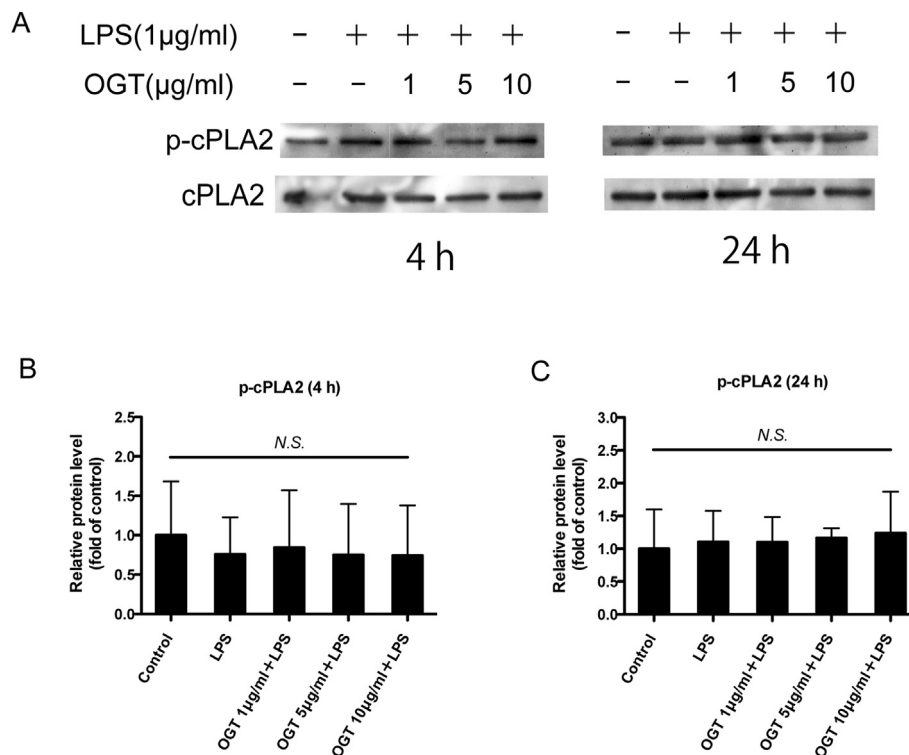

Figure 6. Effects of OGT on cPLA-2 in BV-2 cells. After 4 or 24 h of OGT exposure to BV-2 cells, whole cell lysates were analyzed for phospho or total cPLA2 expression by immunoblot assay (A). Immunoblot quantification of phosphor cPLA2/β-actin are shown in B (4 h) and C (24 h). *N.S.*, not significant.
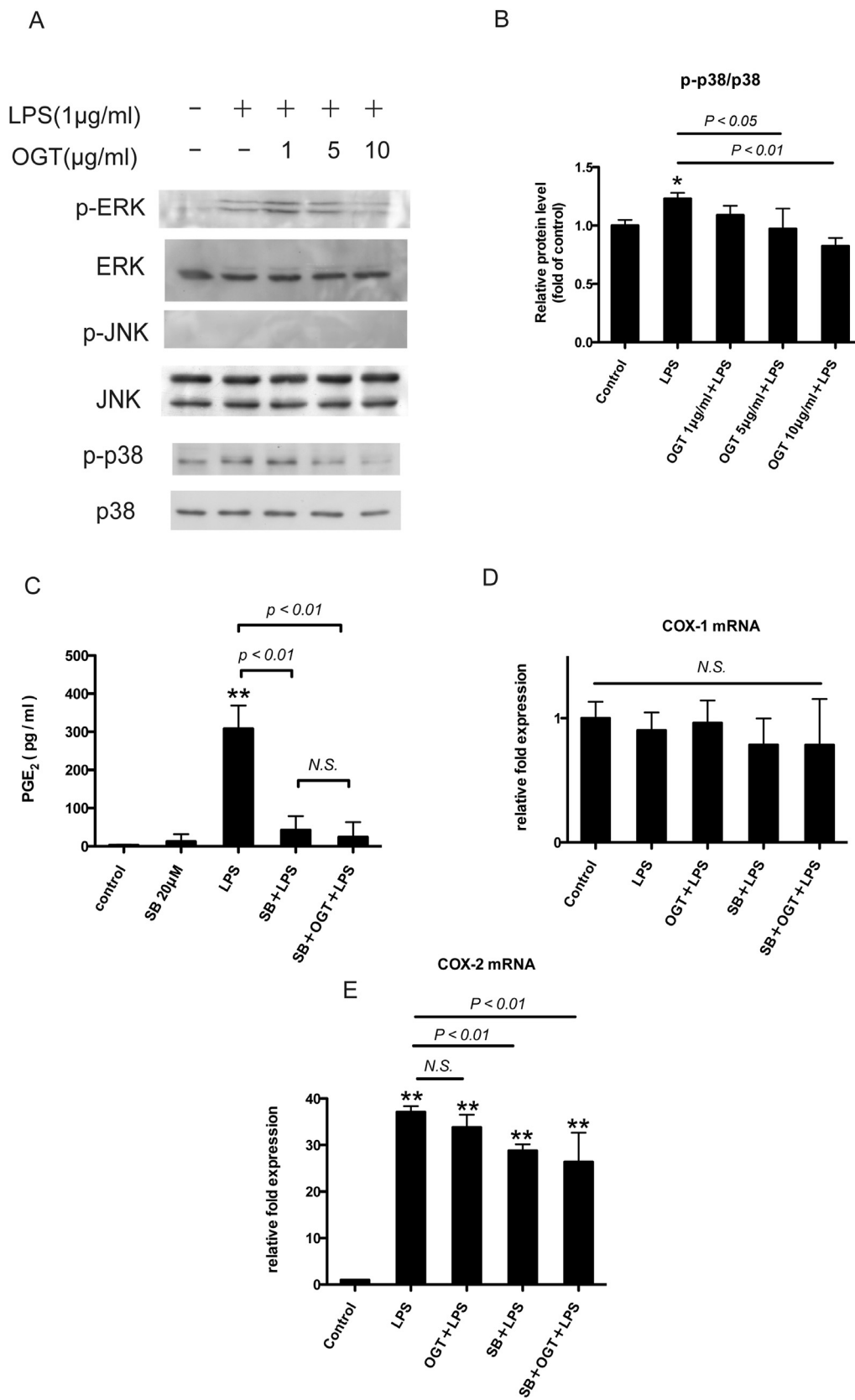
Figure 7. Effects of OGT on MAPKs in BV-2 cells. BV-2 were exposed to LPS (1 μg/ml) with or without OGT for 24 h. Whole cell lysates were analyzed for phosphor-extracellular signal-regulated kinase (p-ERK), ERK, phospho-JNK (p-JNK), JNK, phospho-p38 (p-p38), and p38 MAPK expression by immunoblot assay (A). The figures are representative of at least three independent experiments. Immunoblot quantification of p-p38/p38 MAPK are shown in B. BV-2 microglial cells were exposed to LPS (1 μg/ml) for 24 h with SB203580 (20 μM) or OGT (10 μg/ml) (C–E). The level of PGE2 was analyzed by the enzyme immunoassay. COX-1 (D) and COX-2 (E) mRNA were analyzed using real-time qRT-PCR, normalized to that of 18S rRNA and expressed relative to the mean of control. Data are shown as mean ± S.D. of three independent experiments. **$P < 0.01$ versus control, *$P < 0.05$ versus control, N.S., not significant.
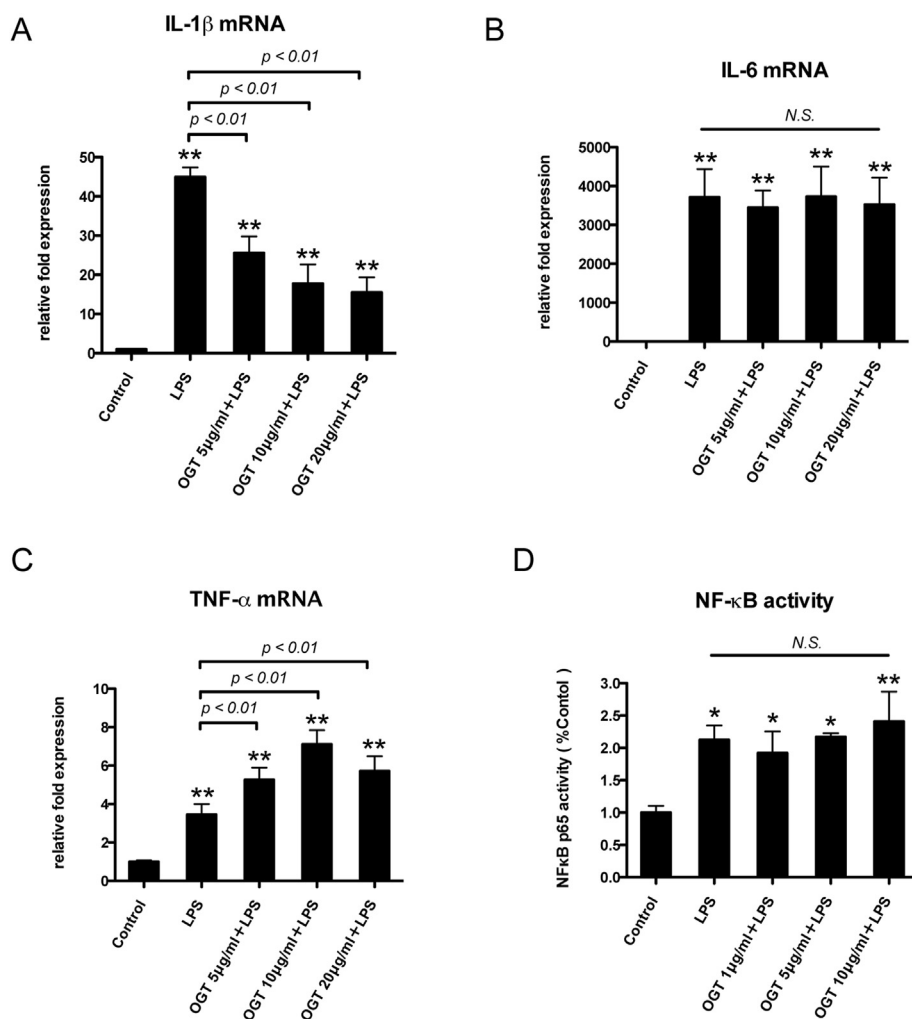
Figure 8. Effects of OGT on proinflammatory cytokine expression and activities on NF-κB in BV-2 cells. BV-2 cells were exposed for 24 h to LPS (1 μg/ml) and OGT at the indicated concentrations. Interleukin (IL)-1β (A), IL-6 (B), and tumor necrosis factor-alpha (TNF-α) (C) mRNA were assayed with real-time RT-PCR. Data are presented as mean ± S.D. of three to five independent experiments. The expression levels of IL-1β, IL-6, and TNF-α were normalized to that of 18S and were expressed relative to the control mean. (D) BV-2 cells were exposed to LPS and OGT for 24 h, and nuclear factor-kappa B (NF-κB) transcriptional activity was measured with an Elisa-based kit. The data are shown as mean ± S.D. of three independent experiments. **$P < 0.01$ versus control, *$P < 0.05$ versus control, *N.S.*, not significant.

the OGT concentration was relatively high (50–200 μg/ml) [24]; therefore, the discrepancy between their study and our study may be due to variations in the experimental settings. In our study, OGT did not affect COX-1 expression, nor did it inhibit COX enzyme activity. These results suggest that OGT functions through the COX-independent pathway in inhibiting PGE2 in BV-2 cells. The COX-dependent pathway has been investigated mainly for elucidating the regulation of PGE2 induction, but little is known about the COX-independent pathway. The current study showed that OGT suppressed p38 MAPK phosphorylation, which has been linked with the regulation of PGE2 production in spinal microglia, especially after nerve injury [25]. p38 MAPK induces the phosphorylation and activation of cPLA2 [26], which in turn controls the release of arachidonic acid (AA) from the cell membrane [27], to be subsequently catalyzed for PGE2 production. However, in our study, OGT did not affect cPLA2 phosphorylation or expression. On the other hand, p38 MAPK has been reported to activate the transcriptional factor NF-κB, which upregulates COX-2 [28]. In the present study, the p38 MAPK inhibitor SB203580 partially suppressed COX-2 induction although the effect was not so distinctive on PGE2 production. In any case, OGT did not suppress the transcriptional activity of NF-κB or COX-2 expression. Therefore, OGT can suppress PGE2 induction via p38 MAPK through an as yet unknown mechanism in addition to regulating COX-2 or cPLA2. However, OGT can still function independently of p38 MAPK regulation. As another possible mechanism in the brain, AA has been reported to be derived from monoacylglycerol lipase (MAGL) in addition to cPLA2 [29]; OGT can act on MAGL.

Furthermore, the organic anion-transporting polypeptide 2Aa 1 (OATP2A1), which controls the extracellular secretion of PGE2, has been strongly expressed in microglia [30]. Thus, the mechanism involved in the PGE2 regulation of OGT possibly involves OATP2A1.

Several activities of PGE2 have been reported in the brain. For example, intracerebral PGE2 is strongly involved in sickness responses such as fever, anorexia, fatigue, and somnolence during infectious diseases [31, 32]. In experiments adopting the sepsis model in mice, PGE2 was induced within hours in astrocytes [33] and cerebral vascular endothelial cells [34]. Sickness-associated behaviors have been reported to be eliminated in EP3, one of the PGE2 receptors, deficient mice [35]. In the current study, we found that OGT suppresses PGE2 induction in LPS-stimulated astrocytes. It has long been known that OGT has an antipyretic effect, but the precise mechanism is unclear. OGT might elicit this through affecting intracerebral PGE2, although the effect of OGT on PGE2 from vascular endothelial cells is unknown. On the other hand, microglia-derived PGE2 is constitutionally produced, and it is reported that part of physiological PGE2 in the brain is derived from microglia [36]. The function of this physiologically produced PGE2 is not well clarified, but it is reported that PGE2 under physiological concentration has the effect of preventing unnecessary inflammation in the brain [36]. In our study, OGT did not influence PGE2 induction in BV-2 cells without LPS stimulation. Conversely, excessive release of PGE2 exerts neurotoxicity and may cause neurodegenerative diseases [37]. For example, Alzheimer's disease (AD) is a chronic neurodegenerative disease causing 60%–70% of dementia and is histopathologically characterized by
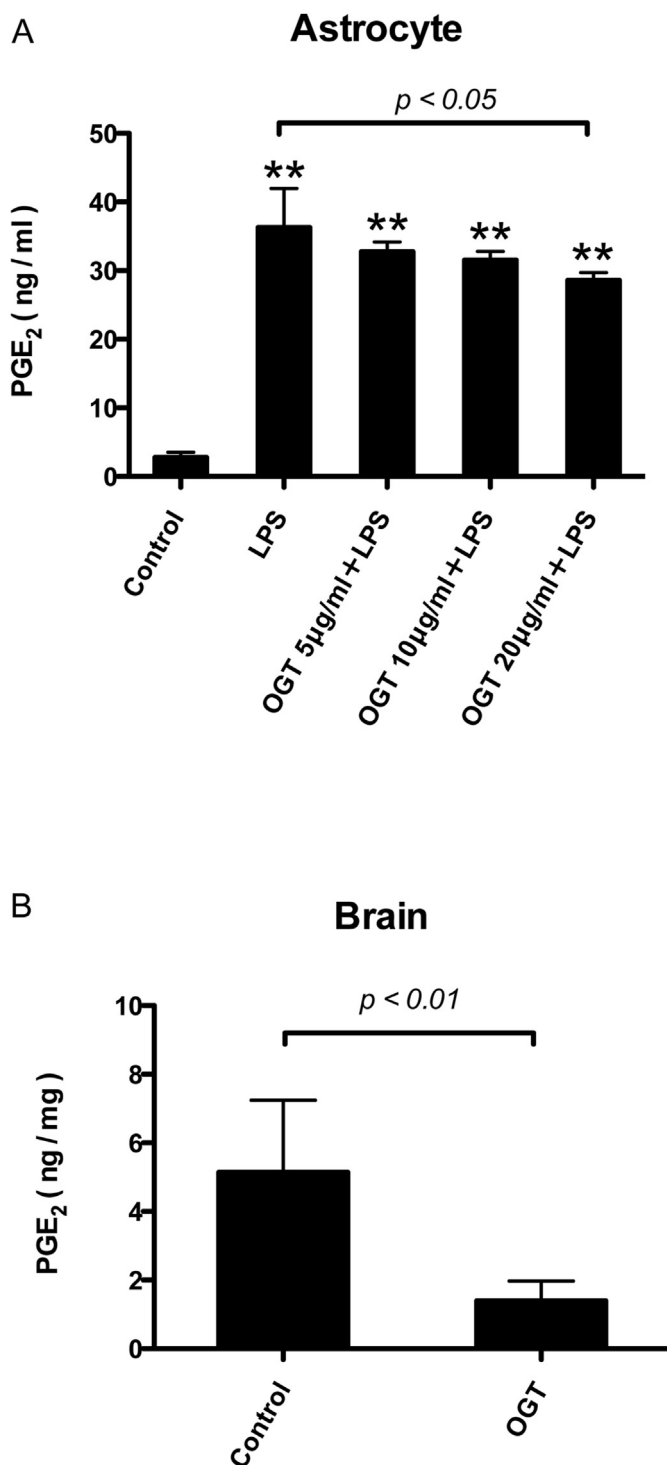
development of AD [40]. In an AD mice model, knockout of EP receptors showed a decrease of amyloid deposits and improvement in cognitive functions [41]. Furthermore, specific knockout of microglial EP2 increased microglial clearance of amyloid β and suppressed neuronal death. PGE2 is now regarded as a promising target. Indeed, NSAIDs have been reported to prevent and delay the development of AD in epidemiologic studies [42]. However, practically, NSAIDs are hardly a good choice for preventing AD because they inhibit the beneficial effects of prostaglandins and induce renal, intestinal, and cardiovascular side effects. In contrast, OGT suppressed PGE2 from activated microglia, and previous study reported that OGT does not affect intestinal PGE2 [12]. Generally speaking, herbal medicines tend to have mild effects and are relatively suitable for long-term administration. It is considered that OGT may be effectively used for the prevention of AD.

When a systemic infection occurs, the microglia is often activated and induces neuroinflammation by producing various inflammatory substances [2, 4]. However, these substances, when over-expressed, can disturb neuronal activities [2]. Patients with sepsis are often complicated with consciousness disorder, a phenomenon known as septic encephalopathy [5]. In the current study, we found that OGT significantly suppressed IL-1β induction in LPS-stimulated microglia. IL-1β secreted by the microglia promotes demyelination of neuronal axons [43] or suppresses anti-inflammatory cytokines like IL-10 and TGF-β [44]. On the other hand, we found OGT upregulated LPS-induced TNF-α induction and ERK phosphorylation, especially at lower concentrations. TNF-α is associated with neural tissue apoptosis and increased inflammation [4]. Therefore, considering proinflammatory cytokines, the effect of OGT is ambivalent and might have a beneficial or detrimental effect against the cytotoxicity of activated microglia.

5. Conclusion

The investigation of the effects of OGT on the induction of inflammatory substances in LPS-stimulated microglial cultured cells BV-2 showed that OGT inhibited IL-1β expression. OGT also suppressed PGE2 induction in a concentration-dependent manner, which was experimentally confirmed using primary culture astrocytes and mice. OGT also did not affect COX expression or activities. These results show that OGT suppresses PGE2 induction in a COX-independent manner in BV-2 microglial cells. It might also exert a beneficial effect against AD or septic encephalopathy, although this needs to be investigated in follow-up studies.

Declarations

Author contribution statement

Yoshika Iwata: Performed the experiments.

Mariko Miyao; Akiko Hirotsu; Kenichiro Tatsumi; Tomonori Matsuyama: Analyzed and interpreted the data; Contributed reagents, materials, analysis tools or data.

Nobuo Uetsuki: Conceived and designed the experiments; Contributed reagents, materials, analysis tools or data.

Tomoharu Tanaka: Conceived and designed the experiments; Analyzed and interpreted the data; Contributed reagents, materials, analysis tools or data; Wrote the paper.

Data availability statement

Data will be made available on request.

Figure 9. PGE2 inhibitory effects of OGT in primary cultured astrocytes and mice brains. Primary cultured astrocytes were exposed to LPS (1 μg/ml) and OGT. The level of PGE2 was analyzed by enzyme immunoassay (A). The data are shown as mean ± S.D. of three independent experiments. **$P < 0.01$ versus control, *N.S.*, not significant. BALB/cCrSlc mice were administered OGT orally 4 g/kg for 4 days; 24 h after LPS (10 mg/kg) injection, mice brains were harvested and PGE2 concentration was quantified (B). Data are presented as means ± S.E. (n = 6).

amyloid plaques and neurofibrillary tangles [38]. Amyloid deposits activate microglia, and the inflammatory responses of microglia are now regarded as one of the major factors exacerbating AD [39]. Especially, COX/PGE2/EP receptor signaling plays important roles in the

Declaration of interests statement

The authors declare no conflict of interest.

Additional information

No additional information is available for this paper.

Acknowledgements

References

[1] F. Ginhoux, S. Lim, G. Hoeffel, D. Low, T. Huber, Origin and differentiation of microglia, Front. Cell. Neurosci. 7 (2013) 45.

[2] J. Gehrmann, Y. Matsumoto, G.W. Kreutzberg, Microglia: intrinsic immuneffector cell of the brain, Brain Res. Rev. 20 (1995) 269–287.

[3] R.N. Christensen, B.K. Ha, F. Sun, J.C. Bresnahan, M.S. Beattie, Kainate induces rapid redistribution of the actin cytoskeleton in ameboid microglia, J. Neurosci. Res. 84 (2006) 170–181.

[4] F. Aloisi, Immune function of microglia, Glia 36 (2001) 165–179.

[5] C.N. Widmann, M.T. Heneka, Long-term cerebral consequences of sepsis, Lancet Neurol. 13 (2014) 630–636.

[6] M. Tsuda, T. Masuda, J. Kitano, et al., IFN-gamma receptor signaling mediates spinal microglia activation driving neuropathic pain, Proc. Natl. Acad. Sci. U. S. A. 106 (2009) 8032–8037.

[7] M.T. Heneka, M.P. Kummer, E. Latz, Innate immune activation in neurodegenerative disease, Nat. Rev. Immunol. 14 (2014) 463–477.

[8] P. Rangarajan, L. Eng-Ang, S.T. Dheen, Potential drugs targeting microglia: current knowledge and future prospects, CNS Neurol. Disord. - Drug Targets 12 (2013) 799–806.

[9] D.H. Gire, K.M. Franks, J.D. Zak, et al., Mitral cells in the olfactory bulb are mainly excited through a multistep signaling path, J. Neurosci. 32 (2012) 2964–2975.

[10] Y.K. Park, Y.S. Chung, Y.S. Kim, O.Y. Kwon, T.H. Joh, Inhibition of gene expression and production of iNOS and TNF-alpha in LPS-stimulated microglia by methanol extract of Phellodendri cortex, Int. Immunopharm. 7 (2007) 955–962.

[11] M. Fukutake, N. Miura, M. Yamamoto, et al., Suppressive effect of the herbal medicine Oren-gedoku-to on cyclooxygenase-2 activity and azoxymethane-induced aberrant crypt foci development in rats, Cancer Lett. 157 (2000) 9–14.

[12] N. Miura, M. Fukutake, M. Yamamoto, et al., An herbal medicine orengedokuto prevents indomethacin-induced enteropathy, Biol. Pharm. Bull. 30 (2007) 495–501.

[13] N. Oshima, Y. Narukawa, N. Hada, F. Kiuchi, Quantitative analysis of anti-inflammatory activity of orengedokuto: importance of combination of flavonoids in inhibition of PGE2 production in mouse macrophage-like cell line J774.1, J. Nat. Med. 67 (2013) 281–288.

[14] K. Fukuda, Y. Hibiya, M. Mutoh, et al., Inhibition by berberine of cyclooxygenase-2 transcriptional activity in human colon cancer cells, J. Ethnopharmacol. 66 (1999) 227–233.

[15] A.L. Bartels, K.L. Leenders, Cyclooxygenase and neuroinflammation in Parkinson's disease neurodegeneration, Curr. Neuropharmacol. 8 (2010) 62–68.

[16] V. Bocchini, R. Mazzolla, R. Barluzzi, et al., An immortalized cell line expresses properties of activated microglial cells, J. Neurosci. Res. 31 (1992) 616–621.

[17] T. Tanaka, S. Kai, T. Koyama, et al., General anesthetics inhibit erythropoietin induction under hypoxic conditions in the mouse brain, PloS One 6 (2011), e29378.

[18] J. Xu, Y. Murakami, K. Matsumoto, et al., Protective effect of Oren-gedoku-to (Huang-Lian-Jie-Du-Tang) against impairment of learning and memory induced by transient cerebral ischemia in mice, J. Ethnopharmacol. 73 (2000) 405–413.

[19] S. Takabuchi, K. Hirota, K. Nishi, et al., The intravenous anesthetic propofol inhibits hypoxia-inducible factor 1 activity in an oxygen tension-dependent manner, FEBS Lett. 577 (2004) 434–438.

[20] M. Murakami, H. Naraba, T. Tanioka, et al., Regulation of prostaglandin E2 biosynthesis by inducible membrane-associated prostaglandin E2 synthase that acts in concert with cyclooxygenase-2, J. Biol. Chem. 275 (2000) 32783–32792.

[21] T. Tanioka, Y. Nakatani, N. Semmyo, M. Murakami, I. Kudo, Molecular identification of cytosolic prostaglandin E2 synthase that is functionally coupled with cyclooxygenase-1 in immediate prostaglandin E2 biosynthesis, J. Biol. Chem. 275 (2000) 32775–32782.

[22] M.A. Ajmone-Cat, A. Nicolini, L. Minghetti, Prolonged exposure of microglia to lipopolysaccharide modifies the intracellular signaling pathways and selectively promotes prostaglandin E2 synthesis, J. Neurochem. 87 (2003) 1193–1203.

[23] K. Arakawa, T. Saruta, K. Abe, et al., Improvement of accessory symptoms of hypertension by TSUMURA Orengedokuto Extract, a four herbal drugs containing Kampo-Medicine Granules for ethical use: a double-blind, placebo-controlled study, Phytomedicine 13 (2006) 1–10.

[24] L. Li, H. Zeng, L. Shan, et al., The different inhibitory effects of Huang-Lian-Jie-Du-Tang on cyclooxygenase 2 and 5-lipoxygenase, J. Ethnopharmacol. 143 (2012) 732–739.

[25] S.X. Jin, Z.Y. Zhuang, C.J. Woolf, R.R. Ji, p38 mitogen-activated protein kinase is activated after a spinal nerve ligation in spinal cord microglia and dorsal root ganglion neurons and contributes to the generation of neuropathic pain, J. Neurosci. 23 (2003) 4017–4022.

[26] R.R. Ji, M.R. Suter, p38 MAPK, microglial signaling, and neuropathic pain, Mol. Pain 3 (2007) 33.

[27] E.A. Dennis, Diversity of group types, regulation, and function of phospholipase A2, J. Biol. Chem. 269 (1994) 13057–13060. PMID: 8175726.

[28] H. Wilms, P. Rosenstiel, J. Sievers, et al., Activation of microglia by human neuromelanin is NF-kappaB dependent and involves p38 mitogen-activated protein kinase: implications for Parkinson's disease, FASEB J. 17 (2003) 500–502.

[29] D.K. Nomura, B.E. Morrison, J.L. Blankman, et al., Endocannabinoid hydrolysis generates brain prostaglandins that promote neuroinflammation, Science 334 (2011) 809–813.

[30] Y. Nakamura, T. Nakanishi, H. Shimada, et al., Prostaglandin transporter OATP2A1/SLCO2A1 is essential for body temperature regulation during fever, J. Neurosci. 38 (2018) 5584–5595.

[31] C.B. Saper, A.A. Romanovsky, T.E. Scammell, Neural circuitry engaged by prostaglandins during the sickness syndrome, Nat. Neurosci. 15 (2012) 1088–1095.

[32] E. Pecchi, M. Dallaporta, A. Jean, S. Thirion, J.D. Troadec, Prostaglandins and sickness behavior: old story, new insights, Physiol. Behav. 97 (2009) 279–292.

[33] R. Hanada, A. Leibbrandt, T. Hanada, et al., Central control of fever and female body temperature by RANKL/RANK, Nature 462 (2009) 505–509.

[34] K. Matsumura, S. Kobayashi, Signaling the brain in inflammation: the role of endothelial cells, Front. Biosci. 9 (2004) 2819–2826.

[35] F. Ushikubi, E. Segi, Y. Sugimoto, et al., Impaired febrile response in mice lacking the prostaglandin E receptor subtype EP3, Nature 395 (1998) 281–284.

[36] S.H. Chen, Y.F. Sung, E.A. Oyarzabal, et al., Physiological concentration of prostaglandin E2 exerts anti-inflammatory effects by inhibiting microglial production of superoxide through a novel pathway, Mol. Neurobiol. 55 (2018) 8001–8013.

[37] S. Bachiller, I. Jimenez-Ferrer, A. Paulus, et al., Microglia in neurological diseases: a road map to brain-disease dependent-inflammatory response, Front. Cell. Neurosci. 12 (2018) 488.

[38] C.K. Glass, K. Saijo, B. Winner, M.C. Marchetto, F.H. Gage, Mechanisms underlying inflammation in neurodegeneration, Cell 140 (2010) 918–934.

[39] N.S. Woodling, Q. Wang, P.G. Priyam, et al., Suppression of Alzheimer-associated inflammation by microglial prostaglandin-E2 EP4 receptor signaling, J. Neurosci. 34 (2014) 5882–5894.

[40] J.U. Johansson, N.S. Woodling, J. Shi, K.I. Andreasson, Inflammatory cyclooxygenase activity and PGE2 signaling in models of Alzheimer's disease, Curr. Immunol. Rev. 11 (2015) 125–131.

[41] F.S. Shie, R.M. Breyer, T.J. Montine, Microglia lacking E Prostanoid Receptor subtype 2 have enhanced Abeta phagocytosis yet lack Abeta-activated neurotoxicity, Am. J. Pathol. 166 (2005) 1163–1172.

[42] C.A. Szekely, J.E. Thorne, P.P. Zandi, et al., Nonsteroidal anti-inflammatory drugs for the prevention of Alzheimer's disease: a systematic review, Neuroepidemiology 23 (2004) 159–169.

[43] E. Zindler, F. Zipp, Neuronal injury in chronic CNS inflammation, Best Pract. Res. Clin. Anaesthesiol. 24 (2010) 551–562.

[44] J.M. Rubio-Perez, J.M. Morillas-Ruiz, A review: inflammatory process in Alzheimer's disease, role of cytokines, Sci. World J. 2012 (2012) 756357.